ADVANCES IN FOREST FIRE RESEARCH

2022

Edited by
DOMINGOS XAVIER VIEGAS
LUÍS MÁRIO RIBEIRO

A Methodology for the Quantitative Risk Analysis of Wildfires in the Wildland-Urban Interface: Application to Electrical Infrastructure

Gonzalo Severino*[1]; Andrés Fuentes[1]; Alejandro Valdivia[2]; Fernando Auat-Cheein[1]; Pedro Reszka[3]

[1]Universidad Técnica Federico Santa María. Avenida España 1680, Valparaíso, Chile, {gonzalo.severino@usm.cl}, {fernando.auat, andres.fuentes}@usm.cl
[2]Chilquinta Distribución S.A. Avenida Argentina N°1, piso 9, Valparaíso, Chile, {avaldivi@chilquinta.cl}
[3]Universidad Adolfo Ibáñez. Diagonal Las Torres 2640, Peñalolén, Chile, {pedro.reszka@uai.cl}

**Corresponding author*

Keywords

Risk, Vulnerability, Consequence, Probit, Wildland-Urban Interface

Abstract

This work describes a methodology to estimate the risk of a wildfire damaging an electrical substation operated by Chilquinta Distribución S.A. (a Chilean utility company) in the Wildland-Urban Interface (WUI) of Valparaiso, Chile. A Wildfire Quantitative Risk Analysis (WFQRA) framework is proposed for this purpose, where risk is defined as the product between the probability of a wildfire reaching the WUI and its consequences. The former is determined with an event tree, a tool where an outcome probability is calculated as the product between the frequency of an initiating event (ignition of a wildland fuel) and the probabilities of passing along a series of intermediate events between the initiating event and the outcome. The intermediate events are burned area > 1 ha, ambient temperature > 22°C, wind velocity > 4 m/s and burn probability > 0.01, for which this event tree anaylsis gives $7.36 \cdot 10^{-5}$ events/year as the probability of a wildfire reaching the WUI. On the other hand, the analysis of consequences requires determining asset vulnerability to a thermal insult, which is the quantitative relationship between thermal exposure of the asset and the damage experienced by it. This vulnerability is assessed by expressing it in terms of a probability of failure (ignition) for different doses of thermal radiation, i.e., a dose-response curve of sigmoid shape. To produce this curve, a probit equation is determined from flammability data of PMMA, a material that served as a proxy for the actual materials within the electrical substation. Thermal exposure of a target within the substation is calculated from fireline intensity and flame length results obtained with FlamMap simulations carried out on a simplified landscape representing the study area along with a simplified model for heat flux from the wildfire front to the target. Ignition probabilities are estimated with this vulnerability model for two wildfire scenarios in the substation. Wildfire risk is thus estimated as 10^{-6} to 10^{-5} events/year, or equivalently, one event every 100,000 to 1,000,000 years.

1. Introduction

Wildfires in Chile have caused significant human, ecological and economic damage to cities, protected areas, and the economy (Reszka and Fuentes 2014; Bowman et al. 2018). Climate change is expected to increase the occurrence and severity of these events (McWethy et al. 2018; Pausas and Keeley 2021; United Nations Environment Programme 2022). A need for tools to address wildfire risk quantitatively has been recognized, to support decision-making for wildfire safety in the Wildland-Urban Interface (WUI) (Finney 2005; Johnston et al. 2020; Miller and Ager 2013; Oliveira et al. 2021), following modern wildfire management paradigms (Moreira et al. 2020).

The goal of this work is to estimate wildfire risk to an electrical substation operated by Chilquinta Distribución S.A., a Chilean utility company. For this purpose, a methodology based on the Quantitative Risk Analysis (QRA) framework (Pasman and Reniers 2014; Center for Chemical Process Safety 2000) is proposed, where risks are defined as the product between the probability of incident outcomes and their consequences. The Wildfire Quantitative Risk Analysis (WFQRA) framework is illustrated in Fig. 1, based on the work by Johnston et al. (2020).

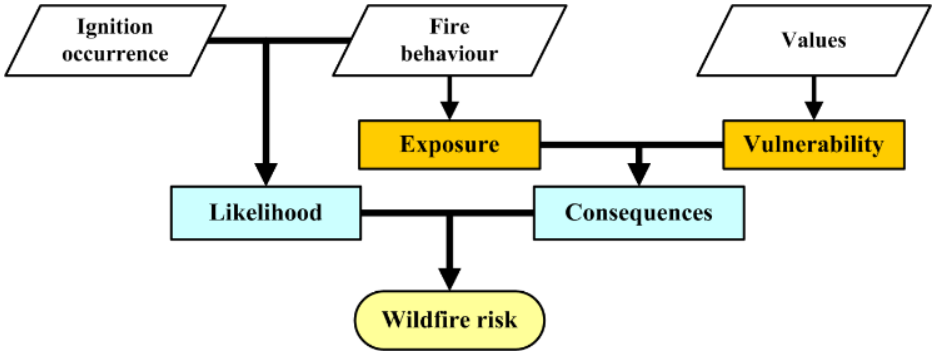

Figure 1- Relations between the definitions adopted for the WFQRA methodology (Johnston et al. 2020).

2. Methodology

The WFQRA can be used to estimate risk at any point of a study area but is used in this work to analyze a small segment of the WUI occupied by the electrical substation. The initiating event of any wildfire is a wildland fuel ignition that develops into sustained combustion of the surrounding fuels. The outcome is the arrival of the wildfire to the WUI. Risk is thus estimated as:

$$R_{x,y} = P_p P_d \tag{1}$$

where P_p is the probability of a wildfire reaching point (x,y), and P_d is the probability of a target sustaining a damage, target ignition in this case.

The electrical substation is in the WUI that surrounds the cities of Valparaíso and Viña del Mar (33°06'30"S, 71°33'32"W; Fig. 2a). Fig. 2b shows a Digital Elevation Model (DEM) of the study area, acquired by the ALOS satellite with resolution of 12.5 m per pixel. Maps for slope and aspect (Figs. 2c and 2d) were produced with this DEM. Fig. 3 shows histograms from hourly data recorded by a weather station located near the study area during the entire year 2020. A survey made by the Chilean Forest Service (CONAF) indicates that *Eucalyptus globulus* plantations are the main fuel in the study area.

Calculating the likelihood of a wildfire reaching the WUI (P_p) requires estimating an historic ignition frequency (f_{ig}), and the conditional probability of a wildfire spreading to the WUI ($P_{p|ig}$), which is predicted with an event tree (Andrews and Dunnett 2000). Therefore:

$$P_p = f_{ig} P_{p|ig} = f_{ig} \prod_{j=1}^{N} P_{p|ig,j} \tag{2}$$

where $P_{p|ig,j}$ is the probability of an intermediate outcome after the j-th node in the event tree, and N is the number of nodes in the branch leading to the outcome of interest.

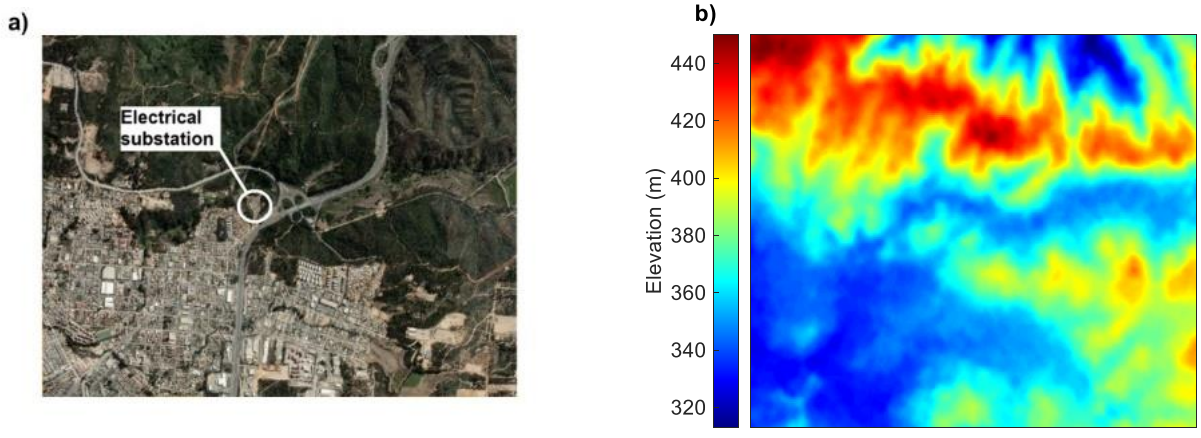

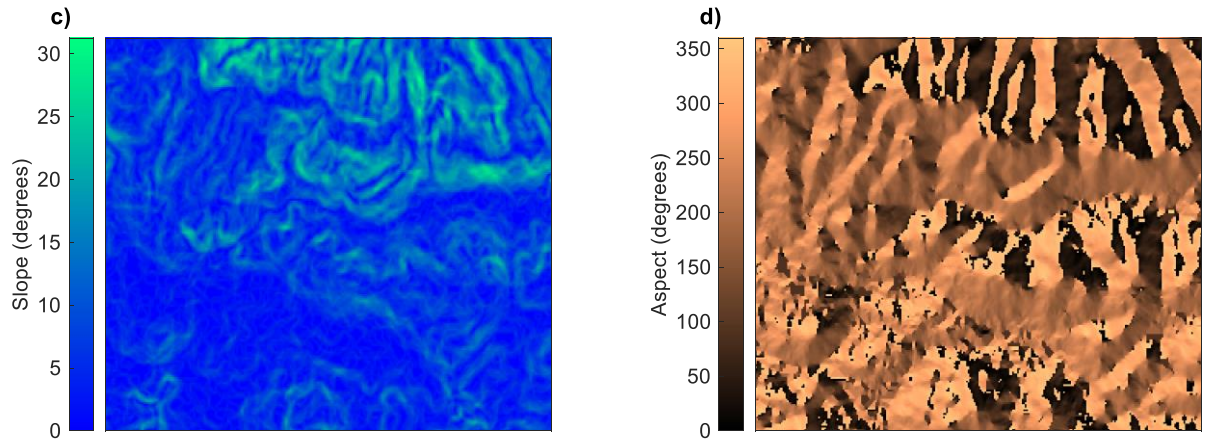

Figure 2- Study area: a) satellite image; b) DEM; c) slope, and; d) aspect map.

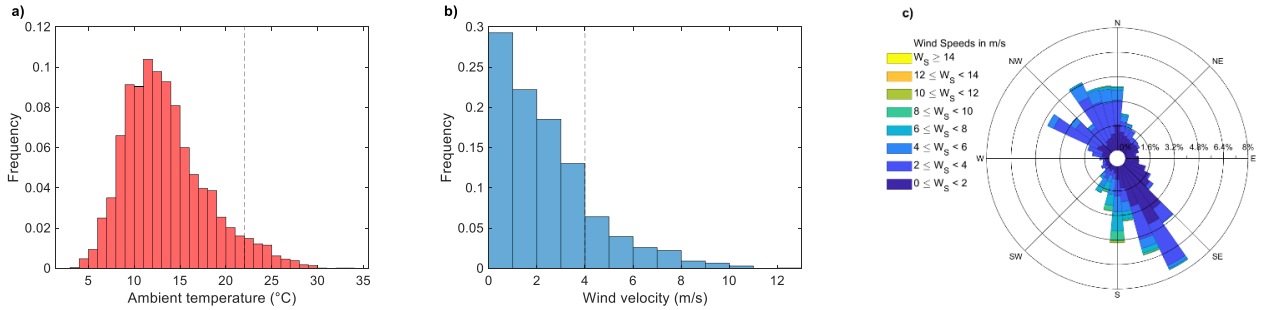

a) ***b)*** ***c)***

Figure 3- Histograms from hourly data recorded by a weather station near the study area during all year 2020: a) temperature; b) wind velocity, and; c) wind rose.

Wildfire consequences depend on both the exposure and the vulnerability of a target to a radiative heat insult. The vulnerability of the target is the quantitative relationship between thermal exposure and target damage. In fires, for damage to occur the target must ignite (a binary response: ignition/no ignition), thus a way of evaluating asset vulnerability is to express it in terms of an ignition probability P_d for different radiant heat fluxes, resulting in a dose-response curve that generally takes a sigmoidal form, which can be converted to a linear function with a probit analysis (Finney 1947). The probit function is the inverse of the cumulative distribution function (CDF) of the standard normal distribution. Therefore, if a dose-response curve is modelled as a normal CDF with mean μ and standard deviation σ, the relation between response P_d and probit variable Y is:

$$P_d(Y) = \frac{1}{\sigma\sqrt{2\pi}} \int_{-\infty}^{Y-5} \exp\left(-u^2/2\right) du \tag{3}$$

where $u = (D-\mu)/\sigma$ and D is a thermal dose. Note that Y is in the upper limit of the integral in the right-hand side of Eq. 3, where 5 is subtracted to Y so that the conversion gives $Y = 5$ when $P_d = 50\%$ (Finney 1947). Since the CDF and its inverse are not available in closed form, computing the probit function requires approximations, e.g.:

$$P_d(Y) = 50\left[1 + \frac{Y-5}{|Y-5|} \cdot \operatorname{erf}\left(\frac{|Y-5|}{\sqrt{2}}\right)\right] \tag{4}$$

By converting the measured cumulative responses into probit variables with Eq. 4, the dose-response curve in terms of the probit variable becomes linearly related to the logarithm of the dose:

$$Y = k_1 + k_2 \cdot \log(D) \tag{5}$$

where k_1 and k_2 are constants from a linear regression. This method is used to evaluate the vulnerability of people (Center for Chemical Process Safety 2000) and vessels (Cozzani et al. 2005) to thermal exposures, and

it is implemented in this work to develop a vulnerability model from flammability data. Considering that electrical equipment is usually manufactured in metallic alloys and polymers, and that the latter are most vulnerable to fires, PMMA is selected as a proxy fuel to develop this model from data available in the literature (Bal and Rein 2011).

For estimating exposure, a configuration consisting of a rectangular solid flame front at some distance from the target within the electrical substation is considered (Fig. 4). Assuming the flame front as a blackbody and neglecting atmospheric transmissivity, radiant heat flux on the target is:

$$\dot{q}_r'' = F\frac{X_r b I_f}{A_f} \tag{6}$$

where F is the view factor between the wildfire front and the target, estimated as described by Morandini et al. (2013), X_r is radiant fraction (assumed equal to 0.3, Pinto et al. 2020), b is rectangle width, H is flame length, A_f is rectangle surface ($A_f = b \cdot H$), and I_f is fireline intensity. Flame length and fireline intensity were determined from FlamMap 6.1 simulations (Finney 2006), using the topography, weather, and fuel models of the study area as inputs. A simplified landscape consisting only of an urban and a wildland area was used for these simulations, with fuel models 91 and 163 from the classification developed by Scott and Burgan (2004) being assigned to these areas. Simulations considered crown fire modeling with constant values for stand height (15 m), canopy base height (1 m) and canopy bulk density (0.2 kg m^{-3}), and a uniform wind field (5 m/s at 150°, cf. Figs. 6d and 3c). Burn probability was also estimated with FlamMap by simulating 1,000 fires ignited at random locations in the study area, considering the same resolution as in the DEM map, crown fire modeling with the same conditions described above, maximum simulation time of 50 min per ignition and spot probability set at 0.5. Although firebrand production is an important pathway for rapid wildfire propagation via spot fires (Fernandez-Pello 2017; Manzello et al. 2020), this phenomenon was not addressed with further detail, since the aim of this work is to demonstrate the usefulness of the WFQRA framework applied to the present case.

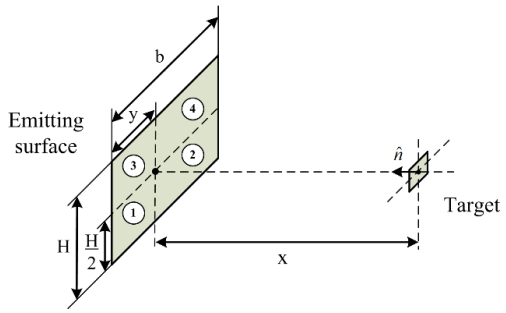

Figure 4- Configuration assumed to determine the view factor between the wildfire front and a differential target.

3. Results

3.1. Likelihood of a wildfire reaching the WUI

Figure 5 shows the event tree proposed to estimate the probability of a wildfire reaching the WUI, which gives P_p = 7.36·10^{-5} events/year. Ignition frequency is estimated at 239 events per year from CONAF historical ignition data circumscribed to the Valparaíso and Viña del Mar municipalities between 2002 and 2019 (Fig. 6a). As this estimation corresponds to the total area of the two cities (52,320 ha), this frequency is scaled down to the study area (996 ha), giving f_{ig} = 239·996/52,320 = 4.55 events per year. Additionally, CONAF has registered the resulting burned areas from these ignitions (Fig. 6b), along with ambient temperature and wind velocity recorded when these ignitions occurred (Figs. 6c and 6d). In the event tree, the probability of a fire resulting in burned area > 1 ha is 0.166 (calculated as 1 – 0.834 = 0.166, where 0.834 is the frequency of burned area between 0 and 1 ha in Fig. 6b), and the probabilities of having representative temperature and wind magnitudes during a wildfire are estimated by selecting their most frequent ranges in the 2002-2019 period (22 to 24°C in Fig. 6c and 4 to 6 m/s in Fig. 6d, respectively), and then summing the frequencies corresponding to temperatures and wind velocities higher than 22°C and 4 m/s in 2020 (Figs. 3a and 3b), giving 0.056 and 0.170, respectively. Figure 7 shows burn probability estimated with FlamMap, from which an average of 0.010 in the substation perimeter is considered for the event tree.

Initiating event	Is burned area > 1 ha	Is ambient temperature > 22°C?	Is wind velocity > 4 m/s?	Burn probability	Outcome
				Yes	Propagation to the WUI
			Yes	0.010	0.0000736
		Yes	0.170	No	No propagation to the WUI
	Yes	0.056		0.990	0.00714
Ignition of a wildland fuel	0.166		No		No propagation to the WUI
4.55			0.830		0.03521
(events/year)		No			No propagation to the WUI
		0.944			0.71239
	No				No propagation to the WUI
	0.834				3.79496

Figure 5- Event tree to estimate the likelihood of a wildfire reaching the WUI.

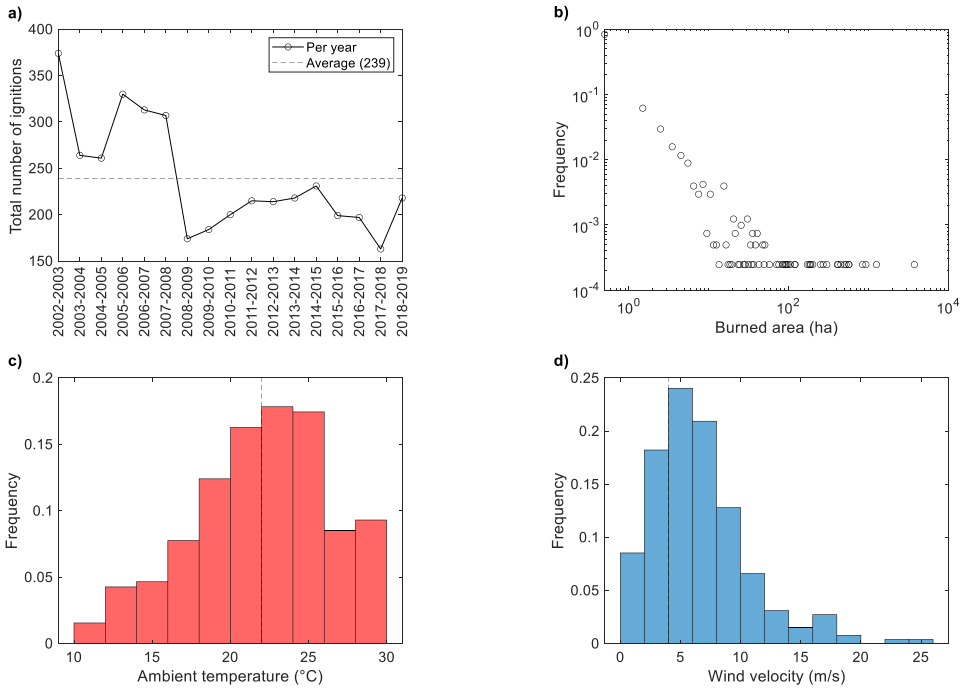

Figure 6- Wildfire data for the Valparaíso and Viña del Mar municipalities between 2002 and 2019: a) ignitions per year (July to June); b) burned area; c) temperature (burned area > 1 ha), and; d) wind velocity (burned area > 1 ha).

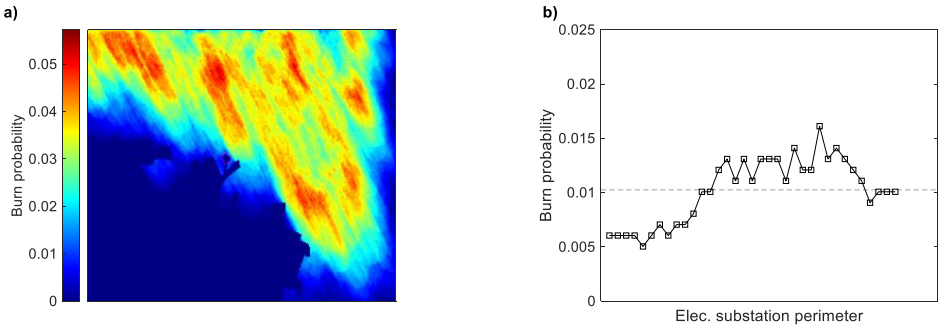

Figure 7- Burn probability: a) map; b) profile in the electrical substation perimeter.

3.2. Vulnerability

A probit equation for the vulnerability of PMMA is determined from the experimental data shown in Fig. 8a (Bal and Rein 2011), where no unique value of a critical heat flux is observed, because these data include results from several authors, heat losses from the specimens induce non-linearities (Sabi et al. 2018, 2021), and a critical heat flux criterion depends on the experimental configuration and procedure (Mindykowski et al. 2011). Instead, there is a transition from a low (~1%) to a high ignition probability (~99%). To estimate the heat fluxes corresponding to these ignition probabilities, it is assumed that data in Fig. 8a is bounded by two curves that tend to these heat fluxes when time to ignition increases:

$$t_{ig,lower} = C_{lower} \cdot (\dot{q}_e'')^{\gamma} \tag{7a}$$

$$t_{ig,upper} = C_{upper} \cdot (\dot{q}_e'')^{\gamma} \tag{7b}$$

where C_{lower} and C_{upper} are two constants, and γ is a common exponent (Sabi et al. 2021). By calculating the logarithm of each side in Eqs. 7a and 7b:

$$\log(t_{ig,lower}) = \log(C_{lower}) + \gamma \cdot \log(\dot{q}_e'') \tag{8a}$$

$$\log(t_{ig,upper}) = \log(C_{upper}) + \gamma \cdot \log(\dot{q}_e'') \tag{8b}$$

Exponent γ is determined with a linear fit to data in Fig. 8b, giving γ = -2.6044. Constants C_{lower} and C_{upper} are estimated by adjusting two bounding curves to the data and determining their intersections with the *y*-axis, giving C_{lower} = exp(12.5) = $2.68 \cdot 10^5$ and C_{upper} = exp(15.3) = $4.41 \cdot 10^6$. With these results, Fig. 8a shows the lower and upper fits to the data expressed by Eqs, 7a and 7b. By setting t_{ig} = 3000 s in Eqs. 7a and 7b, the limiting critical heat fluxes are 5.6 to 16.4 kW/m^2 (dashed lines in Fig. 8a): to the left of this range there is a no-ignition region, and to the right, ignition probability approaches 100%.

Since probit values corresponding to 1% and 99% are 2.67 and 7.33, respectively, a probit equation is obtained by applying a linear fit to these probits as a function of the logarithm of the two limiting heat fluxes (log(5.6) = 1.72 and log(16.4) = 2.80, Fig. 8c), resulting in:

$$Y = -4.8014 + 4.3368 \cdot \log(\dot{q}_e'') \tag{9}$$

Using Eq. 4, Fig. 8d shows ignition probability of PMMA in terms of the logarithm of heat flux.

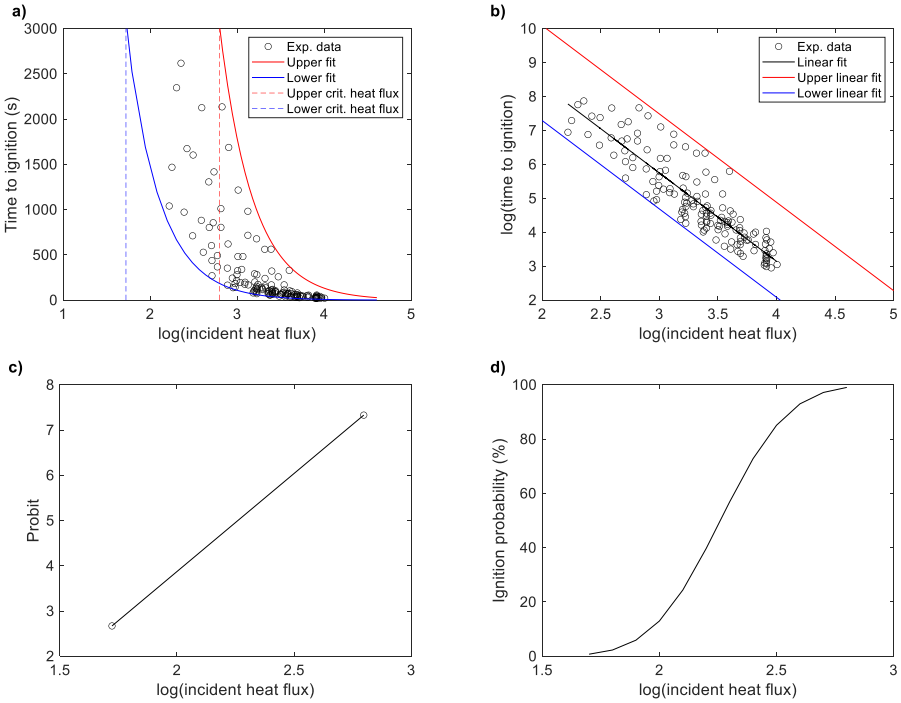

Figure 8- a) Flamambility data used for the PMMA vulnerability model; b) data in log-log scales; c) probit function, and; d) ignition probability.

3.3. Exposure

Fireline intensity and flame length maps from FlamMap simulations are shown in Fig. 9a and 9b. Homogeneous patterns are observed near the WUI, which is attributed to the species uniformity. Fig. 9c and 9d shows fireline intensity and flame length profiles for the substation perimeter, averaging 1832 kW/m and 3.98 m, respectively.

These results represent fire behavior in all the landscape pixels. This is equivalent to a wildfire engulfing the substation perimeter (Fig. 10). A more realistic scenario is a flame front attacking one side of the perimeter at the time. Hence two scenarios are considered (Fig. 10) for estimating view factor and incident heat flux on the target within the substation with Eq. 6, omitting the existence of a wall or fence around it to simplify the problem. Table 1 summarizes these results.

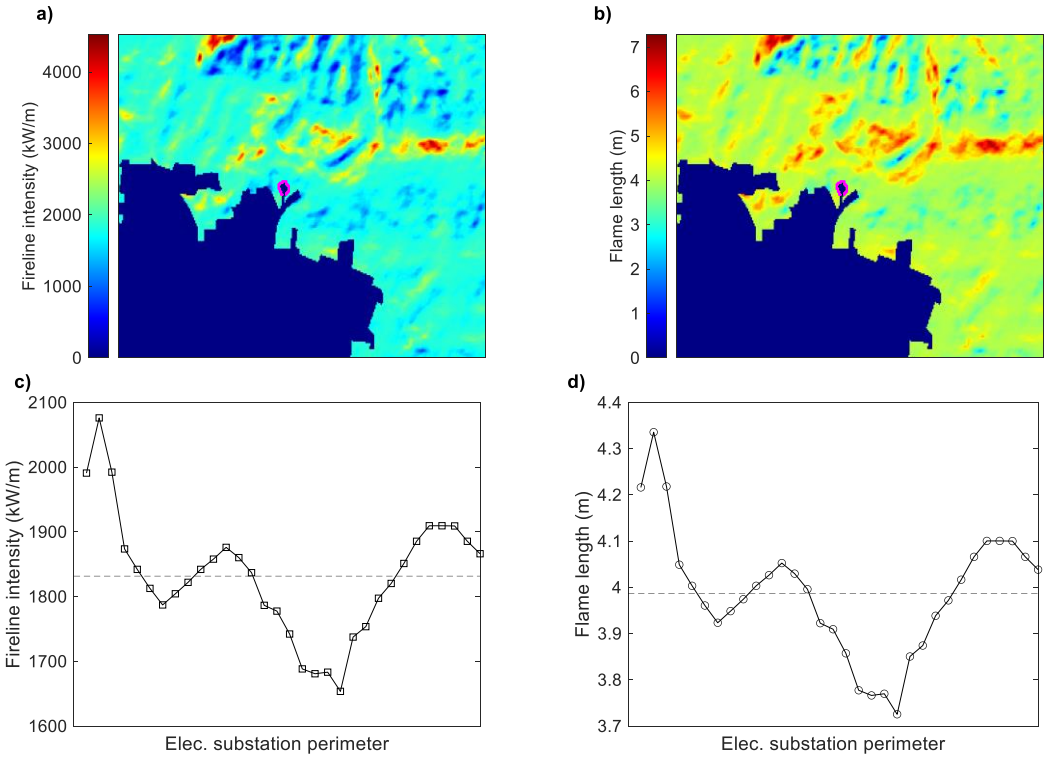

Figure 9- FlamMap outputs: a) fireline intensity; b) flame length; c) fireline intensity profile, and; d) flame length profile.

Figure 10- Scenarios for estimating incident heat flux on a target within the substation. Orange indicates a wildfire engulfing the substation perimeter; yellow rectangles represent the flame fronts considered.

3.4. Wildfire risk

Wildfire risk is calculated with Eq. 1, considering $P_p = 7.36 \cdot 10^{-5}$ events/year (cf. Section 3.1). Probit values are determined with Eq. 9 using the heat fluxes estimated from the fire behavior simulations (cf. Section 3.3), and these probits are used as inputs to Eq. 4 to determine asset ignition probabilities (cf. Table 1). Wildfire risk results are shown in Table 1. Their orders of magnitude are 10^{-6} to 10^{-5} events/year, i.e. one event every 100,000 to 1,000,000 years. It is observed that the probability of a wildfire reaching the electrical substation ($7.36 \cdot 10^{-5}$ events/year) and asset ignition probability (0.03 to 0.3) cannot be used as full risk metrics by themselves only. It is necessary to consider these two components into a wildfire risk estimate, and the definition of wildfire risk proposed in this work is thus more comprehensive than other ones found in the literature (Johnston et al. 2020).

Table 1- Results obtained with the WFQRA for two wildfire scenarios in the electrical substation.

Scenario	A	B
P_p (events/year)	$7.36 \cdot 10^{-5}$	$7.36 \cdot 10^{-5}$
I_f (kW/m)	1832	1832
H (m)	3.98	3.98
b (m)	40	45
A_f (m^2)	159	179
X_r	0.3	0.3
F	0.045	0.060
$\dot{q}_r''$ (kW/m^2)	6.2	8.3
log ($\dot{q}_r''$)	1.82	2.12
Y	3.11	4.38
P_d	0.029	0.269
$R_{x,y}$ (events/year)	$2.2 \cdot 10^{-6}$	$2.0 \cdot 10^{-5}$

4. Discussion

The WFQRA framework presented in this work enables analyzing wildfire risk in a systematic fashion. On one hand, the likelihood of a wildfire reaching the WUI depends on ignition frequency, whose anthropogenic component depends on human behavior and thus could be reduced by educational campaigns, law enforcement or other measures of such nature. This likelihood also depends on burn probability: since a patchy landscape typically hinders wildfire propagation, burn probability could be lowered by treating the wildland fuels and reducing the fuel load near the electrical substation. On the other hand, ignition probability of a target depends mostly on the incident heat flux, which can be lowered by establishing a wide and clear area between the substation and the wildland or blocking radiant heat transfer. Some observations concerning the assumptions, limitations and perspectives of the methodology are:

- Characterizing the study area requires defining a period and spatial delimitation for historical ignition data. Data availability can be an issue because historical records are imperative to estimate ignition frequency. Since climate/weather impacts on the propensity of wildland fuels to ignite, a period of analysis should be clearly and carefully defined so that the estimated ignition frequency be representative of current climatic conditions. Also, the study area may have a particular ignition pattern different to that of the territory in which it is located, hence varying its boundaries for ignition data may also impact on ignition frequency.
- Only two fuel models are considered in this work for simplicity, but a detailed risk analysis requires dividing the study area into several subareas depending on the wildland fuels distribution. This fuel mapping is a challenging task, since it needs a territorial division in terms of plant species, forest type (native or plantation), canopy cover, stand height, fuel load, etc.
- Estimations of flame length and fireline intensity depend on the models incorporated in the fire behavior modeling tool. For example, flame length is usually correlated to fireline intensity via power-law relationships that require two empirical constants, thus flame length might vary one order of magnitude for a given fireline intensity depending on the pair of constants used (Egorova et al. 2022).
- Using a dose-response curve assumes a binary response for the target (ignition/no ignition), in line with a theoretical approach that considers ignition as a phase transition problem where time to ignition either diverges or vanishes according to a universal power-law formula when incident heat flux tends to a critical

value (Sabi et al. 2018, 2021). This approach suits well to understand the sigmoid nature of the dose-response curve for flammability data expressed as ignition probability.

- When the wildfire front arrives to the WUI, firebrands impacting on the target represent a crucial ignition mechanism. Direct thermal radiation and spotting work in parallel, hence the risk posed by them to an asset should be addressed separately, and then summed. Incorporating spotting into the WFQRA framework requires a more extensive database not yet compiled, considering the complex ignition characteristics of structural fuels (Manzello et al. 2020).
- The WFQRA methodology could be used to discriminate between catastrophic and regular wildfires by adding a branch in the event tree to distinguish weather conditions that are prone to extreme fire events from those that are not, leading to two risk estimates, one for regular fires and another for extreme wildfires, which can be directly summed to estimate wildfire risk on the asset.
- In the absence of a tolerability criterion for wildfires, the results obtained with the WFQRA could be compared with risk estimates for other activities. For example, maximum tolerable risks in Canada and the UK are between 10^{-3} and 10^{-6} per year for land-use planning, worker safety and other industries (Muhlbauer 2004).

5. Conclusion

A quantitative methodology for estimating the risk posed by wildfires is proposed and applied to an electrical substation in the WUI of Valparaiso, Chile. Simulations were carried out with FlamMap to estimate burn probability, flame length and fireline intensity in the substation perimeter, but the methodology is independent of the modelling software employed. Wildfire consequences for a proxy fuel within the substation were estimated from a dose-response curve determined with a probit analysis that links incident heat flux on the target with its ignition probability. This comprehensive definition of wildfire risk considers both wildfire occurrence probability (via an event tree analysis) and asset vulnerability, thus potentially enabling a systematic analysis of wildfire risk evolution in time due to climate changes and a quantitative assessment of risk mitigation measures. Due to this, the WFQRA framework is well suited to analyze risk at critical infrastructure located at the WUI.

6. Acknowledgments

This research was jointly funded by ANID SCIA/ANILLO ACT210052 and by Chilquinta Distribución S.A.

7. References

Andrews, J. D., and Dunnett, S. J. (2000). Event-tree analysis using binary decision diagrams. IEEE Transactions on Reliability, 49(2), 230–238. https://doi.org/10.1109/24.877343

Bal, N., and Rein, G. (2011). Numerical investigation of the ignition delay time of a translucent solid at high radiant heat fluxes. Combustion and Flame, 158(6), 1109–1116. https://doi.org/10.1016/J.COMBUSTFLAME.2010.10.014

Bowman, D. M. J. S., Moreira-Muñoz, A., Kolden, C. A., Chávez, R. O., Muñoz, A. A., Salinas, F., González-Reyes, Á., Rocco, R., de la Barrera, F., Williamson, G. J., Borchers, N., Cifuentes, L. A., Abatzoglou, J. T., and Johnston, F. H. (2018). Human–environmental drivers and impacts of the globally extreme 2017 Chilean fires. Ambio, 48(4), 350–362. https://doi.org/10.1007/S13280-018-1084-1

Center for Chemical Process Safety. (2000). Guidelines for Chemical Process Quantitative Risk Analysis (2nd ed.). Wiley-Interscience.

Cozzani, V., Gubinelli, G., Antonioni, G., Spadoni, G., and Zanelli, S. (2005). The assessment of risk caused by domino effect in quantitative area risk analysis. Journal of Hazardous Materials, 127(1–3), 14–30. https://doi.org/10.1016/J.JHAZMAT.2005.07.003

Egorova, V. N., Trucchia, A., and Pagnini, G. (2022). Fire-spotting generated fires. Part II: The role of flame geometry and slope. Applied Mathematical Modelling, 104, 1–20. https://doi.org/10.1016/J.APM.2021.11.010

Fernandez-Pello, A. C. (2017). Wildland fire spot ignition by sparks and firebrands. Fire Safety Journal, 91, 2–10. https://doi.org/10.1016/j.firesaf.2017.04.040

Finney, D. J. (1947). Probit Analysis. Cambridge University Press.

Finney, M. A. (2005). The challenge of quantitative risk analysis for wildland fire. Forest Ecology and Management, 211(1–2), 97–108. https://doi.org/10.1016/j.foreco.2005.02.010

Finney, M. A. (2006). An Overview of FlamMap Fire Modeling Capabilities. In P. L. Andrews and B. W. Butler (Eds.), Fuels Management-How to Measure Success: Conference Proceedings (pp. 213–220). Fort Collins, CO. U.S. Department of Agriculture, Forest Service, Rocky Mountain Research Station.

Johnston, L. M., Wang, X., Erni, S., Taylor, S. W., McFayden, C. B., Oliver, J. A., Stockdale, C., Christianson, A., Boulanger, Y., Gauthier, S., Arseneault, D., Wotton, B. M., Parisien, M. A., and Flannigan, M. D. (2020). Wildland fire risk research in Canada. Environmental Reviews, 28(2), 164–186. https://doi.org/10.1139/er-2019-0046

Manzello, S. L., Suzuki, S., Gollner, M. J., and Fernandez-Pello, A. C. (2020). Role of firebrand combustion in large outdoor fire spread. Progress in Energy and Combustion Science, 76, 100801. https://doi.org/10.1016/j.pecs.2019.100801

McWethy, D. B., Pauchard, A., García, R. A., Holz, A., González, M. E., Veblen, T. T., Stahl, J., and Currey, B. (2018). Landscape drivers of recent fire activity (2001-2017) in south-central Chile. PLOS ONE, 13(8), e0201195. https://doi.org/10.1371/JOURNAL.PONE.0201195

Miller, C., and Ager, A. A. (2013). A review of recent advances in risk analysis for wildfire management. International Journal of Wildland Fire, 22(1), 1–14. https://doi.org/10.1071/WF11114

Mindykowski, P., Fuentes, A., Consalvi, J. L., and Porterie, B. (2011). Piloted ignition of wildland fuels. Fire Safety Journal, 46(1–2), 34–40. https://doi.org/10.1016/j.firesaf.2010.09.003

Morandini, F., Perez-Ramirez, Y., Tihay, V., Santoni, P. A., and Barboni, T. (2013). Radiant, convective and heat release characterization of vegetation fire. International Journal of Thermal Sciences, 70, 83–91. https://doi.org/10.1016/j.ijthermalsci.2013.03.011

Moreira, F., Ascoli, D., Safford, H., Adams, M. A., Moreno, J. M., Pereira, J. M. C., Catry, F. X., Armesto, J., Bond, W., González, M. E., Curt, T., Koutsias, N., McCaw, L., Price, O., Pausas, J. G., Rigolot, E., Stephens, S., Tavsanoglu, C., Vallejo, V. R., Van Wilgen, B. W., Xanthopoulos, G. and Fernandes, P. M. (2020). Wildfire management in Mediterranean-type regions: paradigm change needed. Environmental Research Letters, 15(1), 011001. https://doi.org/10.1088/1748-9326/AB541E

Muhlbauer, W. K. (2004). Pipeline risk management manual: ideas, techniques, and resources (3rd ed.). Elsevier.

Oliveira, S., Rocha, J., and Sá, A. (2021). Wildfire risk modeling. Current Opinion in Environmental Science and Health, 23, 100274. https://doi.org/10.1016/J.COESH.2021.100274

Pasman, H., and Reniers, G. (2014). Past, present and future of Quantitative Risk Assessment (QRA) and the incentive it obtained from Land-Use Planning (LUP). Journal of Loss Prevention in the Process Industries, 28, 2–9. https://doi.org/10.1016/J.JLP.2013.03.004

Pausas, J. G., and Keeley, J. E. (2021). Wildfires and global change. Frontiers in Ecology and the Environment, 19(7), 387–395. https://doi.org/10.1002/FEE.2359

Pinto, P., Cabrera, A., Cruz, J. J., Contreras, J., Severino, G., Demarco, R., Elicer-Cortés, J. C., and Fuentes, A. (2020). Effects of wildland fuel moisture content on radiant heat flux emitted by a laminar non-premixed flame. Applied Thermal Engineering, 181, 115968. https://doi.org/10.1016/j.applthermaleng.2020.115968

Reszka, P., and Fuentes, A. (2014). The Great Valparaiso Fire and Fire Safety Management in Chile. Fire Technology, 51(4), 753–758. https://doi.org/10.1007/S10694-014-0427-0

Sabi, F. Z., Terrah, M. S., Mosbah, O., Dilem, A., Hamamousse, N., Sahila, A., Harrouz, O., Zekri, N., Kaiss, A., Clerc, J.-P., Rahli, O., Giroud, F., and Picard, C. (2018). Ignition/non ignition phase transition. In Advances in Forest Fire Research 2018 (pp. 506–513). Imprensa da Universidade de Coimbra. https://doi.org/10.14195/978-989-26-16-506_55

Sabi, F. Z., Terrah, S. M., Mosbah, O., Dilem, A., Hamamousse, N., Sahila, A., Harrouz, O., Boutchiche, H., Chaib, F., Zekri, N., Kaiss, A., Clerc, J. P., Giroud, F., and Viegas, D. X. (2021). Ignition/non-ignition phase transition: A new critical heat flux estimation method. Fire Safety Journal, 119, 103257. https://doi.org/10.1016/J.FIRESAF.2020.103257

Scott, J. H., and Burgan, R. E. (2005). Standard fire behavior fuel models: a comprehensive set for use with Rothermel's surface fire spread model. U.S. Department of Agriculture, Forest Service, Rocky Mountain Research Station. General Technical Report RMRS-GTR-153. https://doi.org/10.2737/RMRS-GTR-153

United Nations Environment Programme. (2022). Spreading like Wildfire: The Rising Threat of Extraordinary Landscape Fires. A UNEP Rapid Response Assessment.